Effect of sensory blind zones on milling behavior in a dynamic self-propelled particle model

Jonathan P. Newman*
Department of Bioengineering, Georgia Institute of Technology, Atlanta, Georgia, 30332, USA

Hiroki Sayama†
Department of Bioengineering, Binghamton University, State University of New York, Binghamton, New York 13902, USA
and New England Complex Systems Institute, Cambridge, Massachusetts 02138, USA

(Received 20 November 2007; revised manuscript received 22 March 2008; published 22 July 2008)

Emergent pattern formation in self-propelled particle (SPP) systems is extensively studied because it addresses a range of swarming phenomena that occur without leadership. Here we present a dynamic SPP model in which a sensory blind zone is introduced into each particle's zone of interaction. Using numerical simulations, we discovered that the degradation of milling patterns with increasing blind zone ranges undergoes two distinct transitions, including a spatially non-homogeneous transition that involves cessation of particles' motion caused by broken symmetries in the interaction fields. Our results also show the necessity of nearly complete panoramic sensory ability for milling behavior to emerge in dynamic SPP models, suggesting a possible relationship between collective behavior and the sensory systems of biological organisms.

DOI: 10.1103/PhysRevE.78.011913 PACS number(s): 87.19.lp, 05.65.+b, 45.50.−j, 87.18.Ed

Self-organization and pattern formation in self-propelled particle (SPP) systems has been a topic of great interest in theoretical physics, mathematical biology, and computational science [1,2]. It is well understood that the emergence of cohesive swarming motions requires neither leaders nor globally enforced organizational principles. Various SPP models have been used to explore the stability and phase transitions of swarming patterns in response to varying noise levels [3–5] and other control parameters [6–9], as well as to characterize distinct regimes in the parameter space [6,9–11]. Effort has also been allotted to addressing biological questions concerning swarming behavior [7,8,12–16] and to designing nontrivial swarming patterns from combinations of different kinetic parameter sets [17].

SPP models may be classified into two distinct categories: kinematic and dynamic [11]. Kinematic SPP models typically assume that each particle maintains a speed and orientation in accord with its local neighbors [1]. In these models, particles are required to maintain a minimal or constant absolute velocity [1,3,12,13]. Kinematic models have been used for computational modeling of collective behavior of constantly moving groups, such as bird flocks, often implementing empirically constructed complex, spatially discrete interaction zones and behavioral rules that reflect perceptional or locomotive properties of the species being modeled [12–16]. Dynamic SPP models describe the motion of particles using differential equations based on Newtonian mechanics that involve self-propulsion and pairwise attraction and/or repulsion forces [4]. It is known that such models may robustly form coherent milling patterns from initially random conditions even without explicit alignment rules [4,5,9–11]. Dynamic models have been used for both analytical and numerical research on collective behavior of interacting particles in general, with minimal complexity assumed in the particles' intrinsic behaviors.

Here we consider a dynamic SPP model in which a sensory blind zone is introduced into each particle's zone of interaction. Although the assumption of sensory blind zones has been widely adopted in kinematic SPP models [12–16], it has not been considered within a dynamic framework. Specifically, we examine the effect of the sensory blind zones on coherent milling behavior in dynamic SPP models. In doing so, we discovered a transition that occurred with an increasing range of blind zones, and found the system to be highly sensitive to this type of perturbation.

Our model describes the movement, within an open, two-dimensional, continuous space, of N self-propelled particles driven by soft-core interactions whose dynamics are given by

$$\frac{dx_i}{dt} = v_i, \tag{1}$$

$$m\frac{dv_i}{dt} = (\alpha - \beta|v_i|^2)v_i - \nabla U_i(x_i), \tag{2}$$

$$U_i(x) = \sum_{j\neq i} u(|x - x_j|), \tag{3}$$

$$u(r) = C_r e^{-r/l_r} - C_a e^{-r/l_a} \quad (r \geqslant 0), \tag{4}$$

where x_i and v_i are the position and the velocity of the ith particle ($i=1,\ldots,N$), respectively; m the unit mass of one particle; α and β the coefficients of propulsion and friction, respectively; $U_i(x)$ the interaction potential surface for the ith particle; $u(r)$ the pairwise interaction potential function [Fig. 1(a)]; C_r and C_a the amplitudes of repulsive and attractive pairwise interaction potentials, respectively; and l_r and l_a the characteristic ranges of repulsive and attractive pairwise interaction potentials, respectively. Equation (2) includes a velocity-dependent locomotory term and an interaction term achieved through a generalized Morse pairwise interaction potential. This rule set has been employed, with some math-

*jnewman6@gatech.edu
†sayama@binghamton.edu

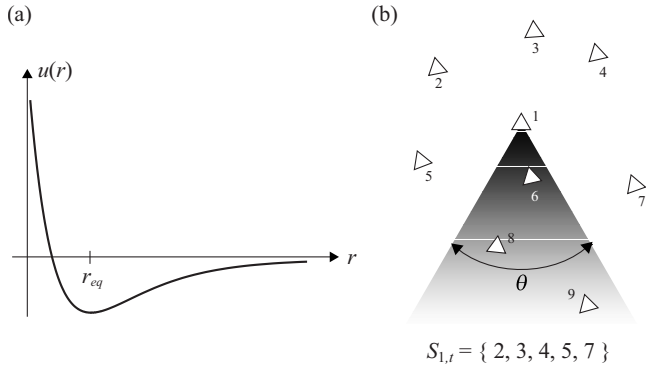

FIG. 1. Model assumptions used in the SPP model employed by this study. (a) Shape of the pairwise interaction potential function $u(r)$ defined by Eq. (4), where r is the distance between two particles. This study explores the biologically relevant regime of parameter settings, in which particles will accelerate away from neighbors who are closer than, and toward neighbors further away than, the equilibrium distance $r_{\mathrm{eq}} \equiv [l_a l_r/(l_a - l_r)]\ln(C_r l_a/C_a l_r)$ (≈ 1.39 with parameter settings used in this paper). (b) A sensory blind zone oriented opposite the direction of forward motion of the particle with angular range θ. Particles are represented by small triangles. In this example, particles 6, 8, and 9 are within particle 1's blind zone, so their indices are not included in the set $S_{1,t}$ when generating repulsive or attractive forces acting on particle 1.

ematical variation, by many previous studies [5,9–11]. In this study, the shape of the pairwise interaction potential falls within the biologically relevant regime defined as $C_r/C_a > 1$ and $l_r/l_a < 1$, as described by [9,11]. Under these parameters, particles rapidly approach an equilibrium velocity of magnitude $v_{\mathrm{eq}} \equiv \sqrt{\alpha/\beta}$ and the system will converge toward a structure for which total dissipation is zero and particles are driven only by conserved forces [9]. In the biologically relevant regime, individuals tend to move toward other individuals that are further from, and away from individuals that are closer than, some critical distance from themselves. This rule is generally applicable to the kinetics of many different biological species and natural systems [2,14,18].

We compare two experimental parameters in the above model: the magnitude of stochastic force (noise) γ and the range of sensory blind zones θ, the former analyzed in [5] and the latter our original extension. Sensory blind zones are incorporated into the design of each particle to mimic the abilities of anisotropic sensory systems observed in nature, such as vision. A sensory blind zone is assumed to exist for each particle with an angular range θ in a direction opposite to the direction of forward motion [Fig. 1(b)].

The inclusion of these parameters introduces discrete events into the model, i.e., abrupt changes of velocity by stochastic force and entry and exit of other particles into and out of sensory blind zones. Consequently, we revised the equations of motion using discrete time steps. The difference equations used for numerical simulation are

$$\frac{x_{i,t+\Delta t} - x_{i,t}}{\Delta t} = v_{i,t+\Delta t}, \tag{5}$$

$$m\frac{v_{i,t+\Delta t} - v_{i,t}}{\Delta t} = (\alpha - \beta|v_{i,t}|^2)v_{i,t} - \nabla U_{i,t}(x_{i,t}) + \gamma\xi_{i,t}, \tag{6}$$

$$U_{i,t}(x) = \sum_{j \in S_{i,t}} u(|x - x_{j,t}|), \tag{7}$$

where $x_{i,t}$ and $v_{i,t}$ are the position and the velocity of the ith particle at time t, respectively; $\xi_{i,t}$ a randomly oriented vector with length 1 whose orientation is independent for each evaluation; $U_{i,t}(x)$ the interaction potential surface for the ith particle at time t; and $S_{i,t}$ the set of indices of all the particles whose positions are outside the blind zone of the ith particle at time t [Fig. 1(b)].

We conducted simulations of this model to produce a milling pattern similar in structure to those witnessed in schools of teleost fish, insects, and microorganisms [2,6,7,9,11,14,19]. Specific values of fixed parameters are as follows: $m=1.0$, $C_r=1.0$, $C_a=0.5$, $l_r=0.5$, $l_a=2.0$, $\alpha=1.6$, and $\beta=0.5$. The initial conditions of each simulation were such that particles were randomly distributed within a square area of side length $2l_a$, and each particle was randomly oriented with magnitude of velocity randomly chosen from $[0, v_{\mathrm{eq}}]$ as described in [9–11].

The model equations were numerically simulated from $t=0$ to 200 at interval $\Delta t=0.01$. No spatial boundaries were enforced. For simulations recording the effect of stochastic force, γ was varied from 0 to 10 at interval 0.5, while $\theta=0$. For simulations testing the effect of sensory blind zones, θ was varied from 0 to 0.2π at interval 0.01π, while $\gamma=0$. Each parameter setting was simulated using several population sizes $N=200$, 300, 400, and 500. Ten simulation runs were conducted for each condition.

Several metrics were used to characterize the simulation results. These include average absolute velocity V_{abs}, ratio of halting particles H, normalized angular momentum M, and normalized absolute angular momentum M_{abs}, defined as follows (the same or similar metrics were used in [9,11,14]):

$$V_{\mathrm{abs}} = \sum_i |v_i|/N, \tag{8}$$

$$H = |\{i \quad \text{such that} \quad |v_i| < \mu v_{\mathrm{eq}}\}|/N, \tag{9}$$

$$M = \frac{|\Sigma_i r_i \times v_i|}{\Sigma_i |r_i||v_i|}, \tag{10}$$

$$M_{\mathrm{abs}} = \frac{\Sigma_i |r_i \times v_i|}{\Sigma_i |r_i||v_i|}. \tag{11}$$

Here $r_i \equiv x_i - x_c$ where x_c is the swarm's center of mass. To measure H we used 20% of the equilibrium velocity ($\mu=0.2$) as a threshold to determine whether a particle was halting or not. When used comparatively, M and M_{abs} make it possible to distinguish single-mill from double-mill formation, in which two mills rotate with opposite sense around similar, but not identical, centers of mass [9,11]. All the metrics were averaged over the last ten time steps of each simulation.

Figures 2 and 3 depict the processes of structural decay produced by stochastic force and blind zone perturbations on the milling behavior of 500 particles. A transition from milling state to disordered state was induced by increasing the

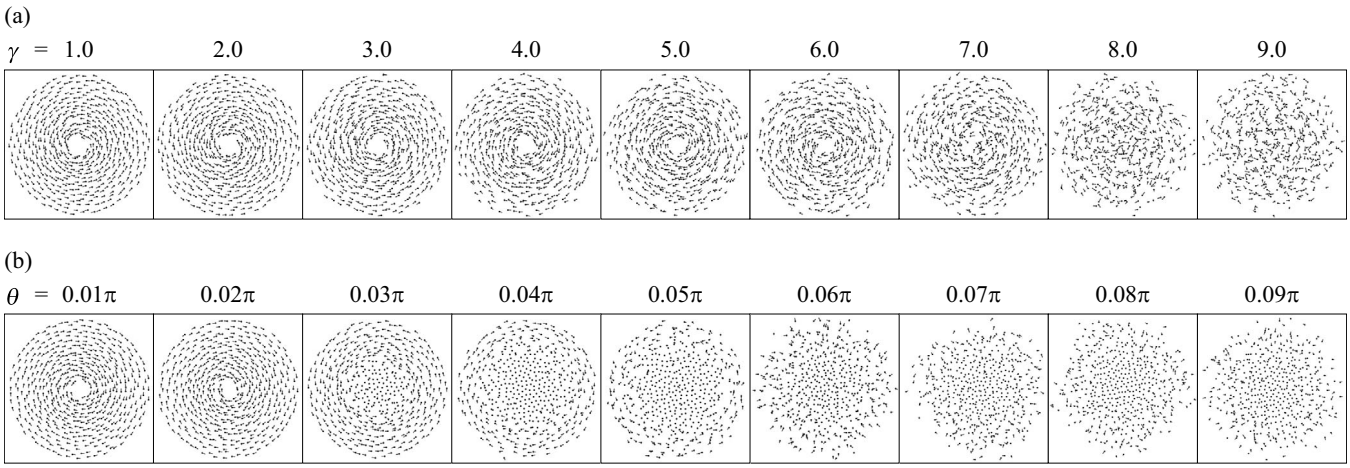

FIG. 2. Visual comparison of the effects of increasing stochastic force and of increasing range of sensory blind zones on the milling behavior of 500 particles. Each image is a final snapshot of a simulated particle swarm taken at $t=200$. Particles have tails that represent the orientation and magnitude of their velocity. (a) Results with increasing stochastic force γ that was varied from 1.0 (left) to 9.0 (right) while $\theta=0$. Transition from milling to disordered states occurred at $\gamma\approx 7.0$. (b) Results with increasing range of sensory blind zones θ that was varied from 0.01π (left) to 0.09π (right) while $\gamma=0$. Transitions from milling to carousel and from carousel to surface-disordered states occurred at $\theta\approx 0.03\pi$ and $\theta\approx 0.06\pi$, respectively. See also Fig. 3.

magnitude of stochastic force across $\gamma\approx 7.0$ [Figs. 2(a) and 3(a)–3(c)]. When the range of sensory blind zones θ was increased, however, structural degradation was very different, involving a spatially heterogeneous transition [Figs. 2(b) and 3(d)–3(f)]. Initiation of collapse occurred at $\theta\approx 0.03\pi$, where particles near the center of the mill ceased rotation and formed a stationary core that has not previously been described to our knowledge. We call this state a "carousel" state. This state is different from the rigid-body rotation reported in [9,11] and the compact but disordered state of [5] because it is characterized by a sharp boundary between the milling surface and the central stationary core made of particles with near-zero velocity [Fig. 3(e)]. A secondary transition was observed across $\theta\approx 0.06\pi$ where the particles moving in the periphery became abruptly disordered and lost coherence in motion while the particles in the central core remained stationary [Fig. 3(f)]. We call this concluding state a "surface-disordered" state.

Particles inside the core in the carousel and surface-disordered states lose their velocity due to a perceptual and consequent force asymmetry. A sensory blind zone creates a longitudinal imbalance between forces derived from particles ahead and forces from particles behind. Because the pairwise equilibrium distance r_{eq} is much longer than the characteristic distance between neighboring particles in a swarm, the imbalance takes effect in the regime of repulsive interactions and thus results in a net resistance against self-propulsion of particles. A particle near the center of the swarm has more particles to its front and back than does a particle rotating in the periphery, since the density of particles is inversely related to the distance from the center of the swarm under the parameter set used here [10] (numerically confirmed in our simulation results; data not shown). Thus, the net resistance against forward motion resulting from the blind zone is larger for particles rotating close to the mill's center. Within a certain distance to the mill's center, the resistance exceeds the range of self-propulsive force possible in Eq. (2), and consequently particles cease motion. This transition does not occur due to increasing γ because the effect of stochastic force is spatially isotropic: it is equally likely to force a particle in any direction and therefore does not lead to cessation of movement.

Figure 4 summarizes all the simulation results, showing the dependence of the final values of V_{abs}, H, M, and M_{abs} on γ, θ, and N. The onset and the mechanism of structural degradation of milling behavior are different for increasing γ and θ. The milling structure is fairly robust to small γ, and it suddenly collapses at $\gamma\approx 7.0$, nearly independently of N. The H plot shows no particles halting in this transition. In con-

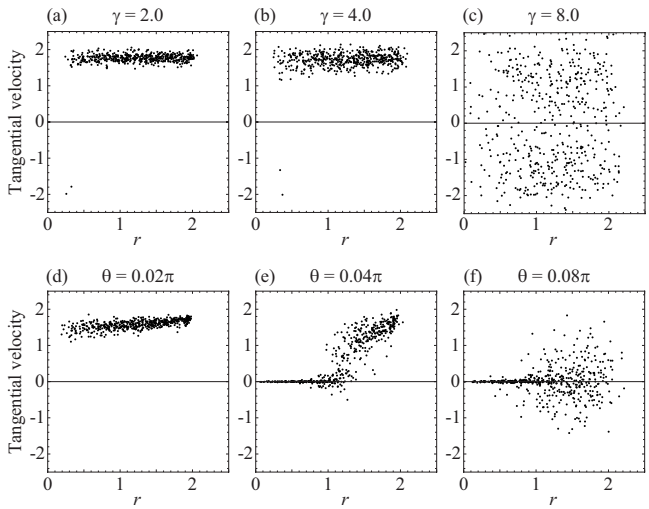

FIG. 3. Tangential velocities of particles plotted over the distance r from the center of mass. Data were obtained from numerical simulations of 500 particles at $t=200$. The direction of rotation of the majority was taken as positive. $\theta=0$ for the top row (a), (b), and (c), while $\gamma=0$ for the bottom row (d), (e), and (f). States of the swarms are as follows: (a) milling, (b) milling, (c) disordered, (d) milling, (e) carousel, and (f) surface disordered.

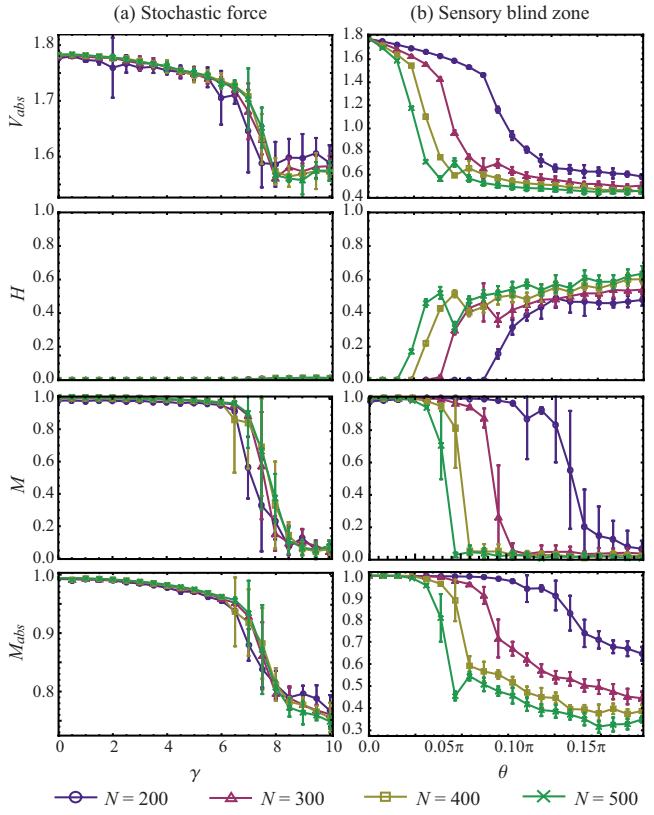

FIG. 4. (Color online) Comparison of the values of the four metrics (average absolute velocity V_{abs}, ratio of halting particles H, normalized angular momentum M, and normalized absolute angular momentum M_{abs}) measured for all simulations for $N=200,300,400,500$. Each data point represents the average of ten simulation runs with an error bar, measured in standard deviations. (a) Results with increasing stochastic force, where the collapse of milling behavior is always reached at $\gamma \approx 7.0$ regardless of N. (b) Results with increasing range of sensory blind zones. The collapse of mill behavior is twofold; the top two plots (V_{abs} and H) capture the first transition from milling to carousel, while the bottom two (M and M_{abs}) capture the second transition from carousel to surface disordered. The critical values of θ for these transitions depend on N, indicating that larger populations are more susceptible to blind zone perturbations.

trast, plots of increasing θ illustrate that structural degradation in increasing θ is a twofold process. The first transition from milling to carousel was detected in V_{abs} and H (emergence of halting particles and consequent decrease of average velocity). The second transition from carousel to surface disordered was detected in M and M_{abs} (loss of coherence in angular momentum). It was also observed in our results that the onsets of these transitions depended significantly on N. This can be understood in that larger N increased the density at the mill's center and made particles more reactive to blind-zone-induced halting.

The blind zone ranges used in these simulations were extremely small from a biological perspective. The largest value tested, $\theta=0.2\pi$, was just 10% of the perception range, which was more than sufficient to destroy milling patterns in all cases. Kinematic SPP models, on the other hand, can produce and maintain milling patterns despite considerable sensory blind zones [14]. To understand this discrepancy in model properties, we note one important difference between kinematic and dynamic frameworks: while particles in kinematic models are always constrained to move with a nonzero velocity, there is a possibility for particles to halt in dynamic models that becomes significant in the presence of rear blind zones like those in our model. This leads us to the hypothesis that milling behavior in an aggregate of organisms may sensitively depend on their ability to maintain constant velocity. Specifically, for organisms that keep moving autonomously at a near constant pace, milling behavior emerges relatively easily even with considerable sensory blind zones. In contrast, for organisms whose motion strongly depends on (either sensory or physical) environmental stimuli, milling behavior requires a nearly complete panoramic range of interaction, especially to perceive the pressure from behind and gain enough forward propulsion to maintain constant velocity.

There are several biological observations that directly or indirectly support our hypothesis. Milling behavior is often reported in groups of microorganisms and insects [2,3,6–10,19]. These organisms rely chiefly on direct physical contact and chemical sensory input, respectively, when forming mills and therefore use omnidirectional sensory capabilities to form aggregates. They also have the ability to cease motion. Additionally, there is a great deal of evidence supporting the isotropic sensory ability of the lateral line in teleost fish [20], some of which demonstrate milling behavior. A recent study that investigated the superficial organization of neuromasts composing the lateral line in goldfish showed that the neuromasts' most sensitive axes were oriented in almost every direction [21]. Moreover, a recent study on Mormon crickets [22] reports that the physical, cannibalistic threat of protein- and salt-deprived individuals from behind plays a critical role in creating a large-scale coherent march. When some crickets are immobilized and therefore unable to respond to a push from behind, the march halts. This study provides clear evidence supporting our conjecture that inputs (physical pressure) from behind a particle can be important in the formation of coherent swarming patterns.

In summary, we computationally studied the effects of sensory blind zones on the stability of self-organizing mill formation in a dynamic SPP model. We found that milling behavior collapses through two spatially distinct transitions in response to an increasing range of rear blind zones, characterized by a halting regime emanating from the center of the swarm and then a disorganization of coherent motion in the periphery area. This is quite different from pattern collapse observed with increasing stochastic force described by a spatially uniform transition to a compact but disordered state [5]. Combined with other results obtained with kinematic SPP models, our results suggest a possible relationship between collective behavior and sensory systems of biological organisms: species that engage in mill formation in nature may have an omnidirectional sensory system if they do not maintain constant velocity by themselves. This is a hypothesis testable and falsifiable through experimental observation.

We thank Boris Chagnaud, Kurt Wiesenfeld, and Stefan Boettcher for their insightful comments on this manuscript.

[1] C. W. Reynolds, Comput. Graph. **21**, 4 (1987).
[2] S. Camazine *et al.*, *Self Organization in Biological Systems* (Princeton University Press, Princeton, NJ, 2003).
[3] T. Vicsek, A. Czirók, E. Ben-Jacob, I. Cohen, and O. Shochet, Phys. Rev. Lett. **75**, 1226 (1995).
[4] U. Erdmann, W. Ebeling, and V. S. Anishchenko, Phys. Rev. E **65**, 061106 (2002).
[5] U. Erdmann, W. Ebeling, and A. S. Mikhailov, Phys. Rev. E **71**, 051904 (2005).
[6] N. Shimoyama, K. Sugawara, T. Mizuguchi, Y. Hayakawa, and M. Sano, Phys. Rev. Lett. **76**, 3870 (1996).
[7] W.-J. Rappel, A. Nicol, A. Sarkissian, H. Levine, and W. F. Loomis, Phys. Rev. Lett. **83**, 1247 (1999).
[8] B. Szabó, G. J. Szölösi, B. Gönci, Zs. Jurányi, D. Selmeczi, and T. Vicsek, Phys. Rev. E **74**, 061908 (2006).
[9] M. R. D'Orsogna, Y. L. Chuang, A. L. Bertozzi, and L. S. Chayes, Phys. Rev. Lett. **96**, 104302 (2006).
[10] H. Levine, W.-J. Rappel, and I. Cohen, Phys. Rev. E **63**, 017101 (2000).
[11] Y.-L. Chuang, M. R. D'Orsogna, D. Marthaler, A. Bertozzi, and L. Chayes, Physica D **232**, 33 (2007).
[12] A. Huth and C. Wissel, J. Theor. Biol. **156**, 365 (1992).
[13] H. Reuter and B. Breckling, Ecol. Modell. **75/76**, 147 (1994).
[14] I. D. Couzin, J. Krause, R. James, G. D. Ruxton, and N. R. Franks, J. Theor. Biol. **218**, 1 (2002).
[15] H. Kunz and C. K. Hemelrijk, Artif. Life **9**, 237 (2003).
[16] C. K. Hemelrijk and H. Kunz, Behav. Ecol. **16**, 178 (2005).
[17] H. Sayama, in *Advances in Artificial Life*, Proceedings of the Ninth European Conference on Artificial Life (ECAL 2007), edited by F. Almeida e Costa, L. M. Rocha, E. Costa, I. Harvey, and A. Coutinho (Springer-Verlag, Berlin, 2007), p. 675.
[18] J. Krause and G. D. Ruxton, *Living in Groups* (Oxford University Press, Oxford, 2002).
[19] J. K. Parrish and L. Edelstein-Keshet, Science **284**, 99 (1999).
[20] R. L. Puzdrowski, Brain Behav. Evol. **34**, 110 (1989).
[21] A. Schmitz, H. Bleckmann, and J. Mogdans, J. Morphol. **269**, 751 (2008).
[22] S. J. Simpson, G. A. Sword, P. D. Lorch, and I. D. Couzin, Proc. Natl. Acad. Sci. U.S.A. **103**, 4152 (2006).